Preliminary Radiological Assessment of the Fusion Ignition Research Experiment (FIRE)

H.Y. Khater and M.E. Sawan

October 1999

UWFDM-1112

FUSION TECHNOLOGY INSTITUTE

UNIVERSITY OF WISCONSIN

MADISON WISCONSIN

Preliminary Radiological Assessment
of the Fusion Ignition Research Experiment (FIRE)

H.Y. Khater and M.E. Sawan

Fusion Technology Institute
Department of Engineering Physics
University of Wisconsin-Madison
1500 Engineering Drive
Madison, WI 53706

October 1999

UWFDM-1112

Preliminary Radiological Assessment
of the Fusion Ignition Research Experiment (FIRE)

H. Y. Khater and M. E. Sawan
Fusion Technology Institute
University of Wisconsin-Madison
1500 Engineering Dr.
Madison, WI 53706

Abstract- Detailed activation analysis has been performed for FIRE**.** The machine is assumed to have an operation schedule of 3000 D-T pulses with a pulse burn of 10 seconds and 2 hours between pulses. At shutdown, the decay heat induced in the first wall is less than 0.1% of the nuclear heating generated in the first wall during operation. The ratio between the shutdown decay heat and nuclear heating generated in the vacuum vessel during operation is on the order of 0.01%. At the end of the machine life, all components would qualify for disposal as Class C low level waste. The biological dose rates behind the vacuum vessel and the divertor remain high during the first year following shutdown. The biological dose rates behind the outboard magnet are acceptable only at locations where the vacuum vessel is more than 40 cm thick. Using a 30 cm thick POLY/CAST shield drops the dose rates on the top of the shield to acceptable levels within a week from shutdown.

INTRODUCTION

Detailed activation analysis has been performed for the Fusion Ignition Research Experiment (FIRE). The FIRE design is conducted as part of the Next Step Options (NSO) activities [1]. A cross section showing the different FIRE components is shown in Fig. 1. FIRE is a compact high field tokamak that utilizes cryogenically cooled copper coils. The current FIRE design has a major radius of 2 m and minor radius of 0.525 m. The design includes a first wall which is 5 cm thick and made of a CuCrZr alloy including a 0.5 cm layer of Be coating. The vacuum vessel structure is made of 316 SS and it uses a mixture of 304 SS and water as a vacuum vessel shield. The vacuum vessel thickness varies poloidally from 5 cm in the inboard region to 57 cm in the outboard region at the midplane. The magnet winding pack is also made of the CuCrZr alloy, which is 60.3 cm thick on the outboard side at the midplane. In this study the winding pack was considered to be CuCrZr as a representative material. The magnet uses a 316 SS coil case with 4 cm front thickness and 6 cm back thickness. The divertor consists of three layers. The front layer is composed of 0.5 cm thick tungsten rods followed by 2 cm of a CuCrZr/water mixture, and 17.5 cm of a 316 SS/water mixture.   The activation analysis has been performed assuming peak neutron wall loadings of 1.8 and 3.6 MW/m^2 for the divertor and outboard first wall, respectively. The machine is assumed to have an operation schedule of 3000 D-T pulses with a pulse burn of 10 seconds and 2 hours between pulses. Waste disposal limits have been calculated for the different components of FIRE using the NRC 10CFR61 and Fetter waste disposal concentration limits. In order to assess the feasibility of hands-on maintenance, biological dose rates were calculated at different locations behind the vacuum vessel and the divertor as a function of time following shutdown.

ACTIVITY AND DECAY HEAT

The neutron flux used for the activation calculations was generated by the discrete ordinates neutron transport code DANTSYS 3.0 [2] along with nuclear data based on the FENDL evaluation [3].   The activation analysis was performed using the activation code DKR-PULSAR2.0 [4]. The code combined the neutron flux with the FENDL/A-2.0 [5] cross section library to calculate the activity and decay heat as a function of time following shutdown. Figures 2 and 4 show the specific activity values for the inboard and outboard regions as a function of time following shutdown, respectively. Figures 3 and 5 show the specific decay heat values for the inboard and outboard regions as a function of time following shutdown, respectively. As shown in the figures, the plasma facing components, first wall on the inboard and outboard sides as well as the divertor, produce the highest levels of specific activity and decay heat. However, the favorable operational schedule allows for the decay of short-lived radionuclides between pulses resulting in low levels of activity and decay heat at shutdown.
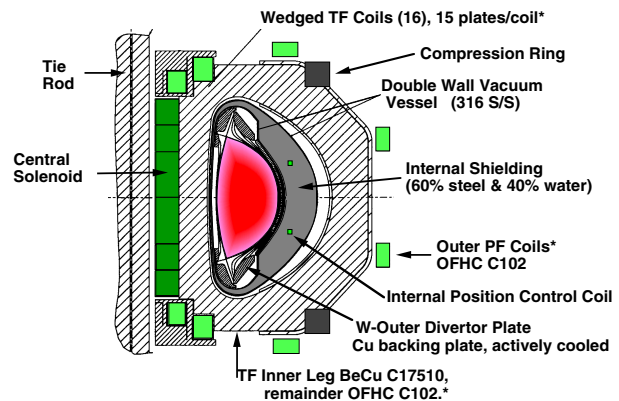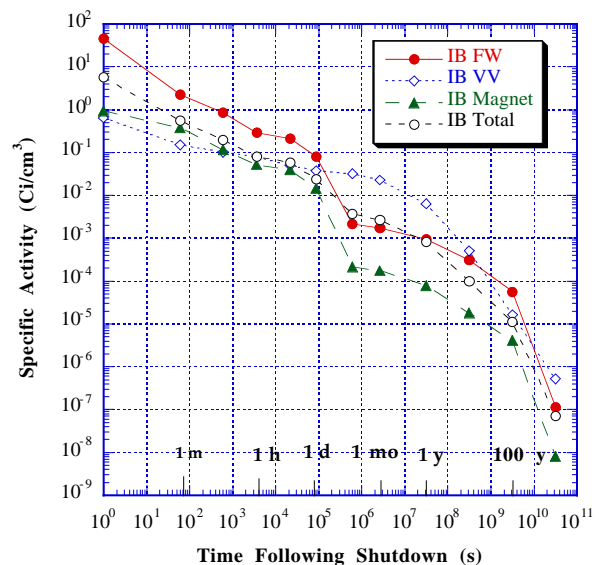

Fig. 1. FIRE components.

Fig. 2. Activity induced in the inboard side.

At shutdown, the decay heat induced in the first wall is less than 0.1% of the nuclear heating generated in the first wall during operation. In the mean time, the ratio between the shutdown decay heat and nuclear heating generated in the vacuum vessel during operation is on the order of 0.01%. The decay heat induced in the first wall at shutdown is dominated by the two copper isotopes ^{62}Cu($T_{1/2}$ = 9.74 min) and ^{66}Cu($T_{1/2}$ = 5.1 min). The low decay heat induced in the first wall at shutdown is due to the fact that the short lifetimes of the ^{62}Cu and ^{66}Cu isotopes allow them to decay during the two hours between pulses. The decay heat induced in the vacuum vessel at shutdown is dominated by ^{52}V($T_{1/2}$ = 3.76 min) and ^{56}Mn($T_{1/2}$ = 2.578 hr) isotopes. Due to the short lifetime of ^{52}V, its entire radioactivity also decays between shots, resulting in a low overall radioactivity generated in the vacuum vessel at shutdown. In general, the short-term activity and decay heat values at shutdown are almost fully dominated by activation during the last pulse. Table 1 shows a list of nuclides that dominate the induced radioactivity in the different machine components.
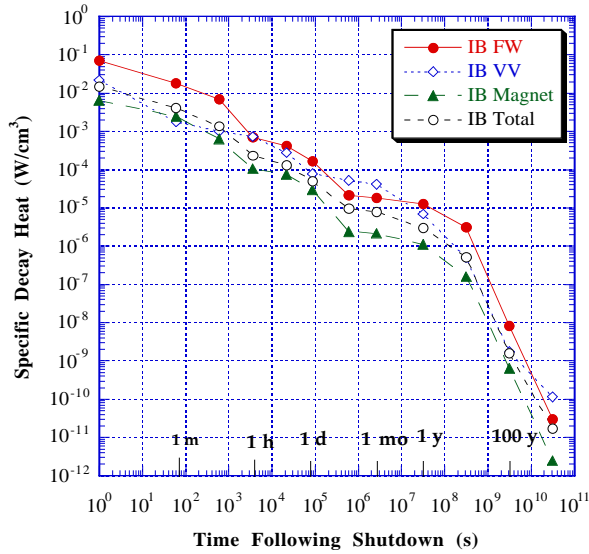

Fig. 3. Decay heat induced in the inboard side.
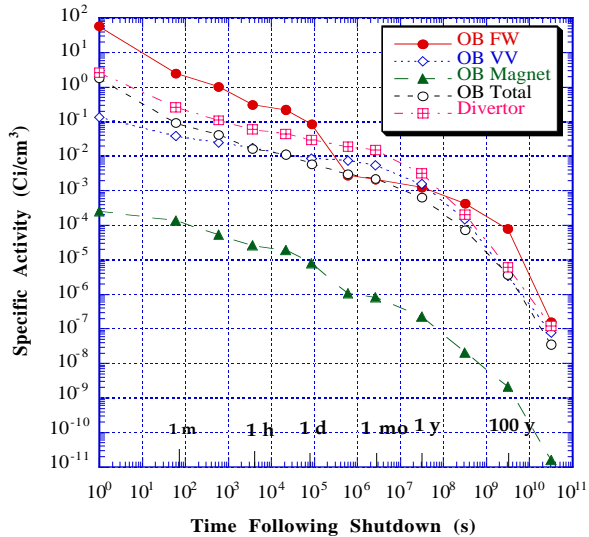

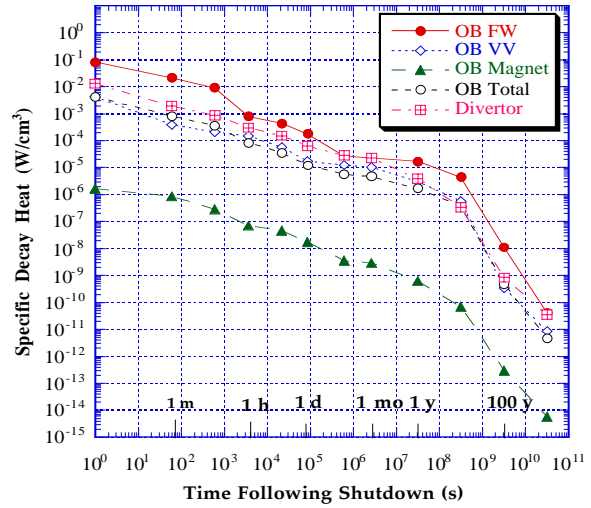Fig. 4. Activity induced in the outboard side and divertor.

Fig. 5. Decay heat induced in the outboard side and divertor.

Table 1. List of Dominant Nuclides.

Short-term< 1 day		
	Activity	Decay Heat
FW	^{62}Cu, ^{64}Cu, ^{66}Cu	^{62}Cu, ^{64}Cu, ^{66}Cu
VV	^{56}Mn, ^{58}Co, ^{51}Cr	^{56}Mn, ^{58m}Co
Mag.	^{62}Cu, ^{64}Cu, ^{66}Cu	^{62}Cu, ^{64}Cu, ^{66}Cu
Div.	^{187}W, ^{185}W, ^{181}W	^{187}W, ^{185}W
Intermediate-term < 1 month		
	Activity	Decay Heat
FW	^{60}Co, ^{63}Ni	^{64}Cu, ^{60}Co
VV	^{55}Fe, ^{51}Cr, ^{57}Co	^{58}Co, ^{54}Mn, ^{58m}Co
Mag.	^{60}Co, ^{63}Ni	^{64}Cu, ^{60}Co
Div.	^{185}W, ^{181}W	^{185}W, ^{181}W
Long-term > 1 year		
	Activity	Decay Heat
FW	^{63}Ni	^{63}Ni
VV	^{63}Ni	^{60}Co, ^{63}Ni
Mag.	^{63}Ni	^{63}Ni
Div.	^{91}Nb, ^{63}Ni	^{94}Nb, ^{39}Ar

BIOLOGICAL DOSE RATES

In order to assess the feasibility of hands-on maintenance, biological dose rates were calculated at different locations following shutdown. The gamma source from radioactive decay was determined at all mesh points and transported, using the DANTSYS 3.0 code, to calculate

the dose rate at different locations following shutdown. The dose rates were calculated at the following locations:

- Behind the outboard vacuum vessel at the midplane.
- Behind the magnet at the midplane.
- Behind the magnet at the machine top.
- Behind the steel/water port plug.
- Behind the shield at the machine top.

Figures 6 and 7 show the biological dose rates at different locations as a function of time following shutdown at the midplane and at the machine top, respectively. As shown in the figures, the biological dose rates behind the vacuum vessel and the divertor remain high during the first year following shutdown. On the other hand, the dose rates behind the magnet and at the midplane are acceptable. Dose rates behind the magnet are caused by the $^{62m}Co(T_{1/2} = 13.9$ min) isotope and are independent of the number of pulses due to the fact that ^{62m}Co decays between pulses. One week following shutdown, the dose rates are dominated by the $^{60}Co(T_{1/2} = 5.27$ yr) isotope. The dose rates caused by the ^{60}Co isotope almost increase linearly with the increase in number of pulses. A steel plug is used to stop neutrons streaming through penetrations. Figure 6 also shows that the dose rates behind the 148 cm long plug are acceptable. A parametric analysis showed that a 110 cm long plug will provide adequate shielding.
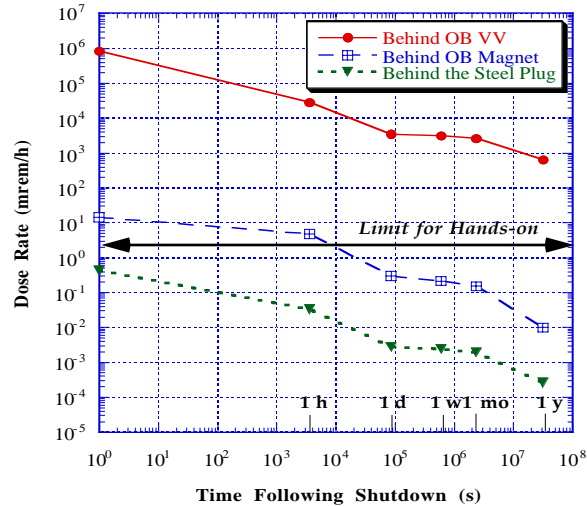

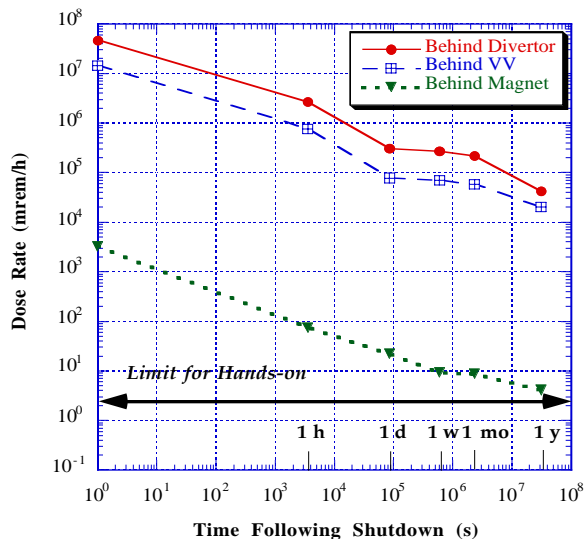Fig. 6. Biological dose rates at the midplane.

Fig. 7. Biological dose rates at the machine top.

The biological dose rates behind the outboard magnet are acceptable only at locations where the vacuum vessel is more than 40 cm thick. The vacuum vessel at the top of the machine is only 12 cm thick. In addition, the magnet at the top of the machine is only 50 cm thick. Even though the 20 cm thick divertor provides the magnet with additional shielding, the biological dose rates behind the magnet at the top of the machine are still high and hence require extra shielding, which has been incorporated in the design. As shown in Fig. 8, using a 30 cm thick POLY/CAST shield drops the dose rates on the top of the shield to acceptable levels within a week from shutdown. The shield is composed of a POLY/CAST mix placed inside a steel tank (the tank wall is 1 cm thick). The activation of the outer wall of the steel tank results in the generation of ^{56}Mn. As shown in the figure, the dose from the $^{56}Mn(T_{1/2} = 2.578$ hr) isotope results in a slightly higher dose (in comparison to the no shield case) outside the 20 cm thick shield during the first few hours following shutdown.
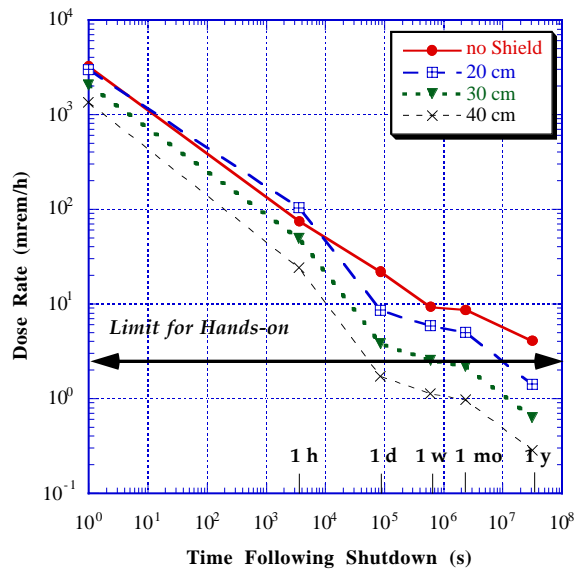

Fig. 8. Biological dose rates at the machine top behind POLY/CAST shield.

WASTE DISPOSAL RATINGS (WDR)

The radwaste of the different components of the machine were evaluated according to both the NRC 10CFR61 [6] and Fetter [7] waste disposal concentration limits (WDL). The 10CFR61 regulations assume that the waste disposal site will be under administrative control for 100 years. The dose at the site to an inadvertent intruder after the 100 years is limited to less than 500 mrem/year. The waste disposal rating (WDR) is defined as the sum of the ratio of the concentration of a particular isotope to the maximum allowed concentration of that isotope taken over all isotopes and for a particular class. If the calculated WDR ≤ 1 when Class A limits are used, the radwaste should qualify for Class A segregated waste. The major hazard of this class of waste is to individuals who are responsible for handling it. Such waste is not considered to be a hazard following the loss of institutional control of the disposal site. If the WDR is > 1 when Class A WDL are used but ≤ 1 when Class C limits are used, the waste is termed Class C intruder waste. It must be packaged and buried such that it will not pose a hazard to an inadvertent intruder after the 100 year institutional period is over. Class C waste is assumed to be stable for 500 years. Using Class C limits, a WDR > 1 implies that the radwaste does not qualify for

3

shallow land burial. Fetter developed a modified version of the NRC's intruder model to calculate waste disposal limits for a wider range of long-lived radionuclides which are of interest for fusion researchers than the few that currently exist in the current 10CFR61 regulations. Fetter's model included more accurate transfer coefficients and dose conversion factors.

The waste disposal ratings for the 10CFR61 and Fetter limits are shown in Table 2. Results in the table are given for compacted wastes. Compacted waste corresponds to crushing the solid waste before disposal and thus disallows artificial dilution of activity. The dominant nuclides are given between brackets. At the end of the machine life, all components would qualify for disposal as Class C low level waste according to the two waste disposal concentration limits used in the analysis. As shown in the table, according to Fetter limits, the WDR are dominated by the silver impurities in the CuCrZr alloy and the niobium impurities in the 316 SS and 304 SS alloys. The 10CFR61 limits indicate that the WDR of components made of the CuCrZr alloy are dominated by ^{63}Ni which is produced from copper by the ^{63}Cu(n,p) reaction. On the other hand, the WDR of components made of the steel alloys are dominated by their niobium impurities.

Table 2. Class C WDR.

Zone	Fetter	10CFR61
IB FW	0.186 (^{108m}Ag)	2.09e-2 (^{63}Ni)
IB VV	4.47e-2 (^{94}Nb)	5.46e-2 (^{94}Nb, ^{63}Ni)
IB Mag.	1.44e-2 (^{108m}Ag)	1.29e-3 (^{63}Ni)
OB FW	0.243 (^{108m}Ag)	2.84e-2 (^{63}Ni)
OB VV	1.82e-3 (^{94}Nb)	3.67e-3 (^{94}Nb, ^{63}Ni)
OB Mag.	7.57e-6 (^{108m}Ag)	3.64e-6 (^{94}Nb, ^{63}Ni)
Plug	7.8e-3 (^{94}Nb)	8.28e-3 (^{94}Nb, ^{63}Ni)
Divertor	2.5e-2 (^{108m}Ag)	1.44e-2 (^{94}Nb)

CONCLUSION

Detailed activation analysis has been performed for the Fusion Ignition Research Experiment (FIRE). The machine is assumed to have an operation schedule of 3000 D-T pulses with a pulse burn of 10 seconds and 2 hours between pulses. The favorable operational schedule allows for the decay of short-lived radionuclides between pulses resulting in low levels of activity and decay heat at shutdown. At shutdown, the decay heat induced in the first wall is less than 0.1% of the nuclear heating generated in the first wall during operation. The ratio between the shutdown decay heat and nuclear heating generated in the vacuum vessel during operation is on the order of 0.01%. Waste disposal limits have been calculated for the different components of FIRE using the NRC 10CFR61 and Fetter waste disposal concentration limits. At the end of the machine life, all components would qualify for disposal as Class C low level waste (LLW) according to the two waste disposal concentration limits used in the analysis. In order to assess the feasibility of hands-on maintenance, biological dose rates were calculated at different locations following shutdown. The results showed that the biological dose rates behind the vacuum vessel and the

divertor remain high during the first year following shutdown. The biological dose rates behind the vacuum vessel and the divertor remain high during the first year following shutdown. The biological dose rates behind the outboard magnet are acceptable only at locations where the vacuum vessel is more than 40 cm thick. Using a 30 cm thick POLY/CAST shield drops the dose rates on the top of the shield to acceptable levels within a week from shutdown.

REFERENCES

[1] "Fire Feasibility Study," Fire Report No. 81_991006_FIREStudy_FT.doc, Rev. 0, October 1999.
[2] R. E. Alcouffe et al., "DANTSYS 3.0, One-, Two-, and Three-Dimensional Multigroup Discrete Ordinates Transport Code system," RSICC Computer Code Collection CCC-547, Contributed by Los Alamos National Laboratory, August 1995.
[3] R. MacFarlane, "FENDL/MG-1.0, Library of Multigroup Cross Sections in GENDF and MATXS Format for Neutron-Photon Transport Calculations," Summary Documentation by A. Pashchenko, et al., Report IAEA-NDS-129, Rev. 3, International Atomic Energy Agency (Nov. 1995).
[4] J. Sisolak, et al., "DKR-PULSAR2.0: A Radioactivity Calculation Code that Includes Pulsed/Intermittent Operation," to be published.
[5] A. Pashchenko et al., "FENDL/A-2.0: Neutron Activation Cross-Section Data Library for Fusion Applications," Report INDC (NDS)-173, IAEA Nuclear Data Section, March 1997.
[6] Nuclear Regulatory Commission, 10CFR part 61, "Licensing Requirements for Land Disposal of Radioactive Waste," Federal Register, FR 47, 57446 (1982).
[7] S. Fetter, E. Cheng and F. Mann, "Long Term Radioactive Waste from Fusion Reactors," Fusion Engineering and Design, 13, 239-246 (1990).